Chapter 5

Design of smartphone based fiber optic evanescent wave sensor for detection of water salinity

---

This chapter discusses the design and working of a smartphone based fiber optic evanescent wave sensor for reliable measurement of water salinity. The chapter describes the issues related to health due to salinity level in water and importance of salinity measurement. Detail theoretical background of evanescent field generation in an optical fiber and its utility to determine salinity level in water has been discussed. Necessary smartphone application has been developed for on-site detection, calibration and data transfer. The chapter ends with the discussion on the the performance of developed sensing system and its usability as an alternative tool over its commercial counterpart.

5.1 Introduction

Salinity is defined as the total dissolved salt content in water [1]. In general, presence of dissolved salt elements such as sodium chloride ($NaCl$), potassium chloride (KCl) and magnesium chloride ($MgCl_2$) in water are responsible for salinity of the medium. The oceanic seawater has salinity value in the range 34 - 35 ppt (parts per thousand) with predominant contribution from sodium (Na^+) (30.6 %) and chloride (Cl^-) (55 %) [2]. Excess content of salinity level in drinking water is considered to be a potential threat for human health. In coastal areas, saline water contamination is often occurred due to seasonal saltwater intrusion from the ocean to groundwater [3]. The saline contamination increases the total sodium ion content in drinking water. Till date no guidelines have been released by WHO regarding the permissible limit of salinity in drinking water, neverthless high level of

salinity may pose numerous direct and indirect health hazard. An epidemiological study carried out by Calabrese et al. [4] revealed that elevated amount of sodium in drinking water contributes to the elevation of blood pressure (BP). Through a survey conducted in 2008, it is hypothesized that saline contamination of drinking water causes higher rates of pre-eclampsia and gestational hypertension in the pregnant women living in coastal areas of Bangladesh as compared to pregnant women living in non coastal region [5]. The hypertension during pregnancy may lead to serious health related consequences such as impaired liver function, low platelet count and maternal deaths [6]. In India nearly 560 million people lives in the Coastal States and Union Territories which are prone to saltwater intrusion [7]. Due to the growing concern of health effect due to high salinity levels in drinking water [8], it is essential to find technological solutions for affordable determination of salinity level in the drinking water. The conventional method for measuring salinity is to measure conductivity of the solution but the electrical conductivity (EC) strongly dependends on temperature [9]. Therefore, a small variation in temperature may lead to a significant variation in the EC value or the corresponding salinity value. Optical techniques based on various fiber optic sensors have been proposed for in-situ monitoring of water salinity [10-13]. Since, refractive index of a medium increases with its salinity level, refractive index based salinity sensors have also been demonstrated [14]. The use of separate opto-electronic components such as laser source, photo-detector, micro-controller and microprocessor make such sensing systems relatively costly and for transfer of in-field data from remote location to central laboratory, a separate communication set-up is needed.

Already discussed in the previous chapters that a smartphone can provide all the necessary requirements from detection, data processing to data transfer facilities which are essential for development of an water quality monitoring system. The direct optical absorbance measurement discussed in chapter 3 may not yield desirable sensitivity in the detection process of salinity in water since it does not form any coloration to the water sample. Fiber optic evanescent wave absorption based sensing can be considered as an alternative technique for the present study due to its high sensitivity for small refractive index variation of salt in water [15]. Gupta et al. [16,17] has demonstrated that U-bent fiber optic configuration enhances the sensitivity of the sensor. Therefore, for development of the proposed smart-

phone based sensing system, the fiber optic evanescent wave sensing principle has been integrated into it. U-bent plastic plastic optical fiber has been considered to develop the sensing region of the sensor. The overall cost can be reduced without sacrificing the sensitivity and robustness of the designed sensor. In almost all previous demonstration of fiber optic evanescent wave sensor requires separate optical sources, detector and external computational facility. Present work demonstrates the potential of applications of fiber optic sensors as a standalone tool for similar purposes. The detailed theoretical background of evanescent wave generation, device fabrication and evaluation of device performance are discussed in the following sections.

5.2 Theory of the fiber optic evanescent wave sensors

When a finite sized light beam is internally reflected from the interface of two dielectric medium, a small portion of the light beam penetrates into the medium of lower refractive index. This phenomena is occurring due to the continuity of tangential components of the incident electromagnetic fields of the light beam. The penetrating field is termed as evanescent wave which is characterized by the following conditions [18]:

1. The amplitude of the wave decreases exponentially from the dielectric boundary and

2. The penetrating wave propagates in a direction parallel to that of the dielectric interface.

The propagation of light in an optical fiber is based on total internal reflection, therefore the generation of evanescent waves at the core-cladding interface is an inherent process [19]. In an optical fiber the evanescent wave propagates parallel to the fiber axis. Figure 5.1 depicts the direction of propagation of the evanescent wave when a light beam is incident at an angle θ greater than that of the critical angle $\theta_c = \sin^{-1}(\frac{n_{cl}}{n_{co}})$ at the core-cladding interface where n_{co} and n_{cl} are the refractive index of core and cladding respectively. The extent up to which the evanescent wave penetrates to a medium is termed as penetration depth (d_p).

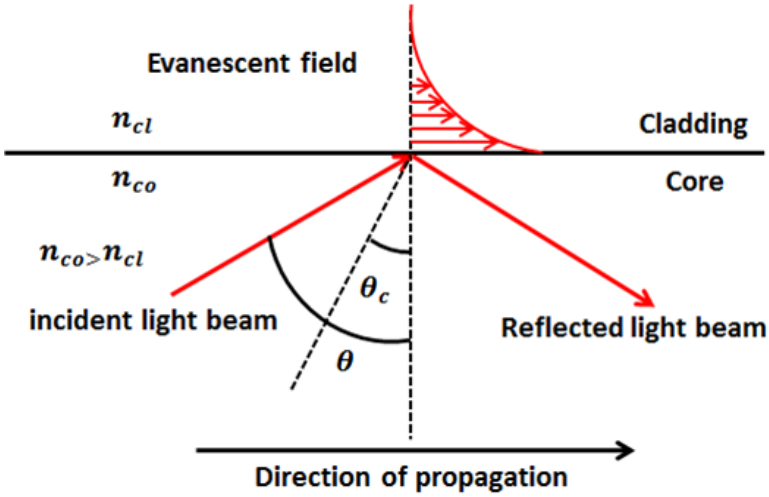

Figure 5.1: Propagation direction of the evanescent wave in a dielectric interface.

It is defined as the perpendicular distance from the dielectric interface at which the evanescent field amplitude decreases by $\frac{1}{e}$ of its value in the interface which is given by the the following equation [16]

$$d_p = \frac{\lambda}{2\pi n_{co}\sqrt{(\sin^2\theta - \sin^2\theta_c)}} \tag{5.1}$$

where, λ is the free space wavelength of the incident light. If the cladding of the optical fiber is removed and replaced by another medium then the penetration depth can be modulated based on the refractive index or concentration of the surrounding medium. This in turn modulates the output light intensity from the optical fiber. If the medium is absorbing then the transmitted light signal also depends on the absorption characteristic of the medium. Thus the concentration can be determined by measuring the output light intensity. This method is called attenuated total reflection (ATR) spectroscopy. The working principle of ATR spectroscopy based sensing scheme has been discussed below. Let us consider a step index multimode optical fiber in which the cladding of length l is locally replaced by an absorbing medium then the power P transmitted by the optical fiber is given by [16]

$$P = P_0.exp(-\gamma l) \tag{5.2}$$

where, P_0 is the power transmitted without the absorbing medium and γ is the evanescent absorption co-efficient of the medium. The evanescent absorption co-

efficient for a ray making an angle θ with the normal to the core-cladding interface is given by [16]

$$\gamma(\theta) = \frac{\alpha\lambda n_2 \cos\theta \cot\theta}{2\pi\rho {n_{co}}^2 \cos^2\theta_c \sqrt{\cos^2\theta_c - \cos^2\theta \sin^2\theta_\phi}} \tag{5.3}$$

where α is the bulk absorption coefficient, ρ is the radius of the core and θ_ϕ is the skewness angle. From equation 5.3 it can be seen that the for a fixed value of θ, $\gamma(\theta)$ becomes maximum when $\theta_\phi = \frac{\pi}{2}$. Thus, considering only the incident meridional rays equation 5.3 becomes

$$\gamma(\theta) = \frac{\alpha\lambda n_2 \cos\theta \cot\theta}{2\pi\rho {n_{co}}^2 \cos^2\theta_c \sqrt{\sin^2\theta - \sin^2\theta_c}} \tag{5.4}$$

Equation 5.4 shows that the value of evanescent coefficient $\gamma(\theta)$ increases with the increase the refractive index of the medium n_2. The refractive index depends on the density of the medium[20]. Since, density of seawater increases with the increase of salinity level [21,22], therefore refractive index variation has been alternatively used to determine the salinity [14]. In the present work, the increase in salinity or more specifically $NaCl$ concentration increases the refractive index (n_2) of the medium which can be correlated to the variation of output light intensity from the optical fiber. This modulated light intensity data can be used to determine the corresponding salinity level in water with the help of a calibration curve.

From equation 5.1 and equation 5.4, it can be seen that both the parameters d_p and γ depends on the angle θ, the angle that the incident light makes with the normal to the core-cladding interface. Decrease in θ eventually increases the value of d_p and γ. For a straight evanescent wave fiber optic sensor θ remains same in the sensing region. Gupta et al. [16] has shown that the angle θ can be decreased in the sensing region by using U-bent configuration in order to enhance the sensitivity. In this particular configuration when the light ray enters the bent sensing region, θ decreases to a new angle which is given by

$$\phi = \sin^{-1}\{(\frac{R+h}{R+2\rho})\sin\theta\} \tag{5.5}$$

where, h is the distance at which the ray is incident on the entrance of the U-shaped probe from the core-cladding boundary and R is the bending radius of the U-shaped probe. Figure 5.2 shows the detailed geometrical configuration of an

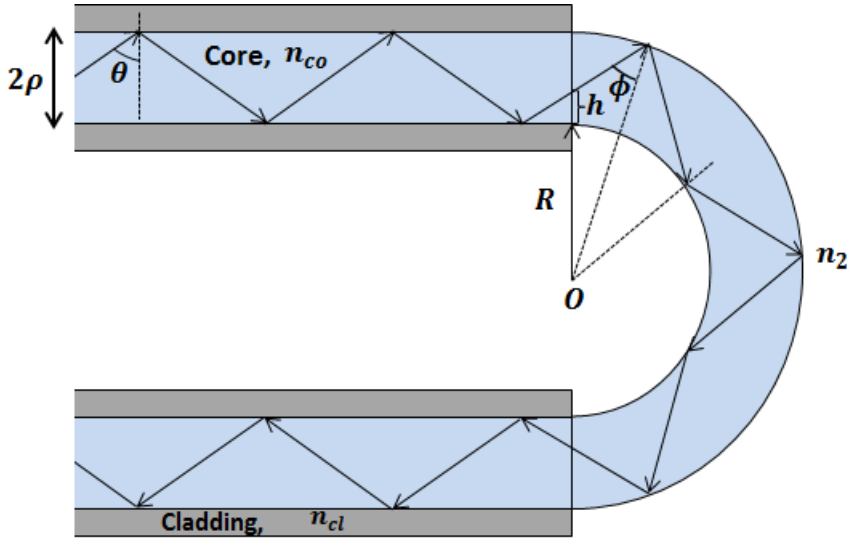

Figure 5.2: U-shaped configuration for enhancing sensitivity of fiber optic evanescent wave sensor.

U-bent fiber optic probe as adopted from [16]. Thus, by reducing the bending radius R, the sensitivity of the fiber optic probe can be enhanced. In the present work, U-bent optical fiber configuration has been considered so that the proposed smartphone sensing system is highly sensitive and capable of measuring small salinity level variations in water samples.

5.3 Materials and methods

At the beginning of this chapter it was stated that sodium and chloride ions are the primary constituents of saline water; therefore in the present work sodium chloride ($NaCl$) are considered for the calibration standards. Laboratory grade $NaCl$ salt has been procured from SRL, India and artificial sea salt (Red sea coral pro salt) has been procured from amazon, India (product no. B00NBI0KW6). Standard saline solutions of different salinity level have been prepared in reagent grade DI water in parts per thousand (ppt) units. The standard solutions have been prepared in three different concentration range: (i) 0 ppt to 1 ppt in step incremental value of 0.1 ppt, (ii) 1ppt to 10 ppt with step incremental value of 1 ppt and (iii) 10 ppt to 100 in step incremental value of 10 ppt. Since, salinity depends on the temperature, therefore during preparation of the samples a constant temperature was maintained. To monitor salinity level in sea water using the designed sensor,

saline solutions of different concentrations have been prepared from the procured artificial sea salt. The artifical salt contains all the minerals which can be found in real oceanic environment. These saline samples have been prepared in the range 5 ppt to 55 ppt with step incremental value of 10 ppt.

5.4 Optical layout and fabrication of the fiber optic sensor

To develop the smartphone based fiber optic sensor, a plastic optical fiber (POF) (Product id. 02534, Edmund optics) of diameter 980/1000 μm with NA 0.51 is used as a sensing probe. In POF, the core is made of acrylic polymer polymethylmethacrylate (PMMA) and the cladding is made of a special thin layer of fluorine polymer. Table 5.1 shows the technical specifications of the POF which has been used in the present work.

Table 5.1: Some important technical specification of the POF

Acceptance Angle (°)	61
Numerical Aperture (NA)	0.51
Core Diameter (μm)	980.00
Fiber Diameter(μm)	1000.00
Core refractive index n_{co}	1.492
Cladding refractive index n_{cl}	1.402
Bend Radius (mm)	25.00

Approximately 20 mm of the POF cladding is removed by polishing it gently with a zero emery paper and then bent in to form a U-shaped probe. As shown in table 5.1, the bend radius of the considered POF is 25 mm. The fabricated POF has been bent to a radius of 50 mm so that the inherent fiber bending loss does not interfere with the considered sensing method. This uncladded U-shaped fiber probe essentially forms the sensing region for the considered smartphone based fiber optic evanescent wave sensor. Figure 5.3 (a) shows the schematic of the designed smartphone based fiber optic evanescent wave sensor. As discussed in chapter 2, the peak spectral response of the embedded ALS is in the wavelength range 600 nm - 700 nm; therefore to get a good sensing response the the optical radiation having peak transmission wavelength within this range is considered as the source of light. The present sensing system has been developed with Sony Xperia E3 smartphone used previously. The LED flash of the smartphone has

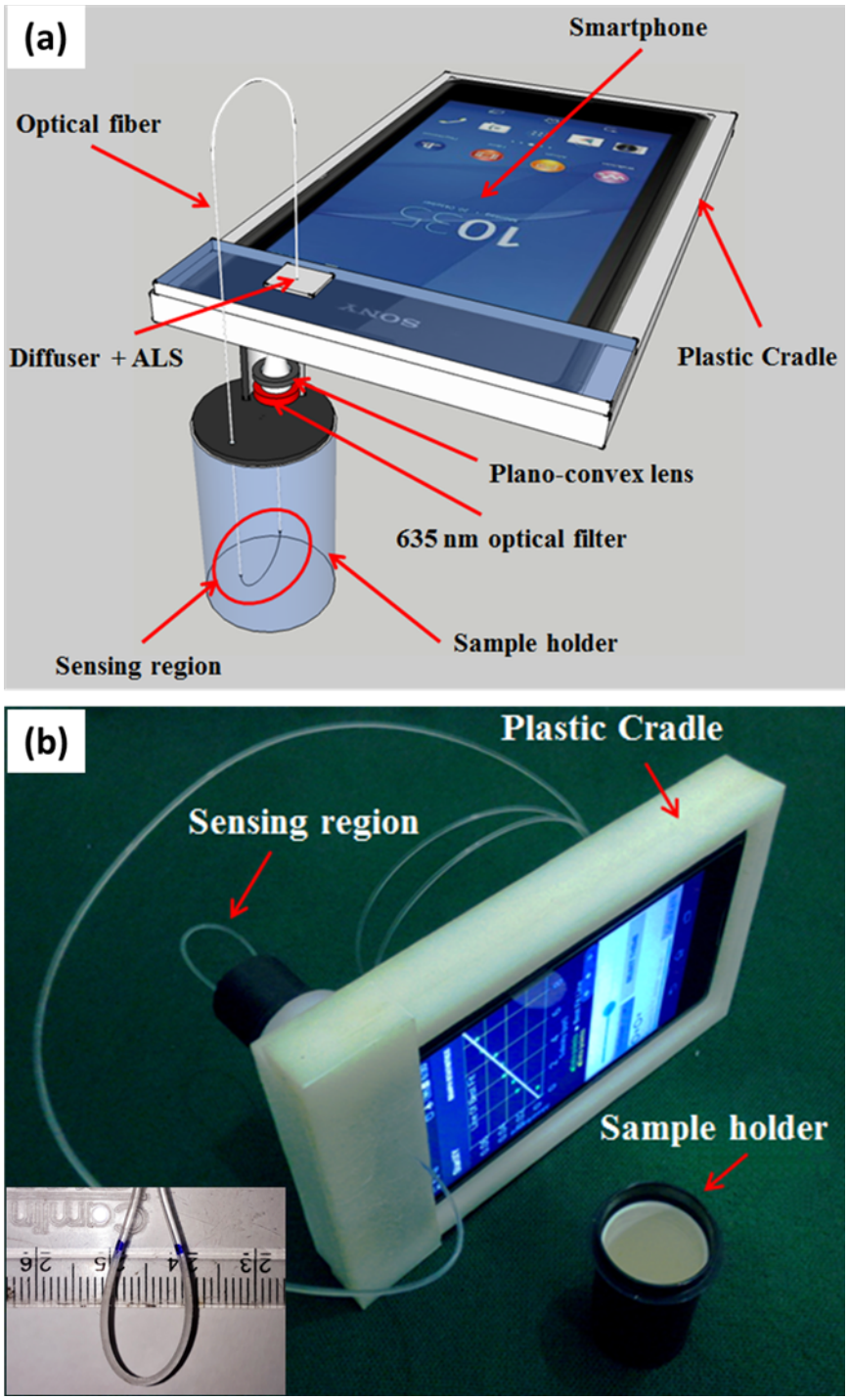

Figure 5.3: (a) Schematic of smartphone based fiber optic evanescent wave sensor and (b) photo image of the designed sensor.

been used as a light source. Using a plano-convex lens the light beam from the LED flash has been collimated and the collimated beam is allowed to propagate through an optical filter with peak transmission wavelength 635 nm. Using a mechanical holder one end of the POF is coupled to the optical filter. The holder has been

fabricated in such a way that it will work as a lid for the blackened sample holder shown in figure 5.3 (a). The embedded LED flash of the considered smartphone is a super bright type white LED which produces high intensity light beam. High intensity creates fluctuations in the ALS reading, therefore in designing the POF sensing system no beam focusing arrangement has been considered to couple the POF to the LED flash. Since, the core diameter of the POF is relatively large (980 μm), therefore light coupling end of the POF is tilted to approximately 60° (the acceptance angle) to that of the collimated light beam so that optimum light signal can propagate through it. The evanescent field at the sensing region of the uncladded POF interacts effectively with the surrounding saline medium and intensity modulation takes place in accordance with the concentration of the sample. The modulated light beam from the POF is received by the smartphone ALS via a diffuser. All optical components including the smartphone have been mounted on a custom designed plastic holder made of Nylon. The inner wall of the Nylon block is blackened so that affect of the ambient light can be neglected. Low cost, high mechanical strength and superior resistance to wear from chemicals make Nylon material a primary choice for fabricating the optical holder in the present investigation. The overall dimension of the setup is measured to be 140 mm in length, 80 mm in breadth and 40 mm in width and the weight of the designed sensor along with the phone is approximately 250 g. The compact nature and low weight promotes the applicability of the device for field sensing applications.

5.5 Development of the android application

To visualize the designed system as a reliable standalone device for water salinity detection purposes, all the necessary detection and data analysis parameters have been implemented in a custom designed android application. As discussed in the chapters III and IV, the already developed detection and data processing algorithms can be implemented in the application with necessary modifications. In the present case, three calibration ranges have been considered. Figure 5.4 shows the screenshots of the developed **SalinitySense** application. Similar to the **TurbiditySense** application developed in chapter 4, the user needs to record the intensity reading for both the sample and the reference (DI water) medium to

determine the corresponding salinity level from a in-built calibration equation by clicking the 'Determine Salinity' button as shown in figure 5.4 (a). The algorithms used previously has been used again for device calibration in the present work.

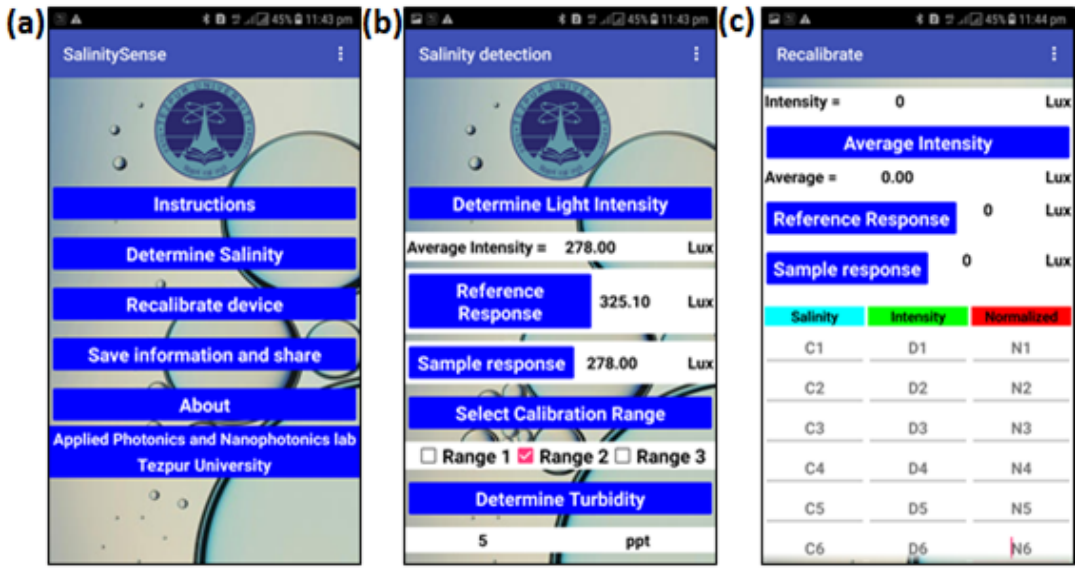

Figure 5.4: Screenshot images of the designed 'SalinitySense' application.

5.6 Device calibration

The designed smartphone based fiber optic sensor has been calibrated with the standard saline samples. In all measurements DI water has been considered as a reference medium. The response of each of the standard saline sample has been recorded for five consecutive times and the average value has been considered for obtaining the calibration curve. All the intensity values has been normalized with the corresponding response of the sensor with the DI water which has been considered as a reference solution with salinity 0 ppt. Figure 5.5 shows the response characteristic of the designed sensor in the salinity range 0 ppt to 100 ppt. It has been observed that the normalized sensor response in the considered salinity range is piece-wise linear. Therefore, in the present work the device has been calibrated in three different salinity range. The responses of each of the considered range are shown in figure 5.6. The coefficient of determination for the considered salinity ranges are found to be $R^2 = 0.984$ for 0 ppt to 1.0 ppt, $R^2 = 0.992$ for 1.0 ppt to 10 ppt and $R^2 = 0.967$ for 10 ppt to 100 ppt. These values suggest that the salinity of any sample in the considered ranges can be measured almost precisely

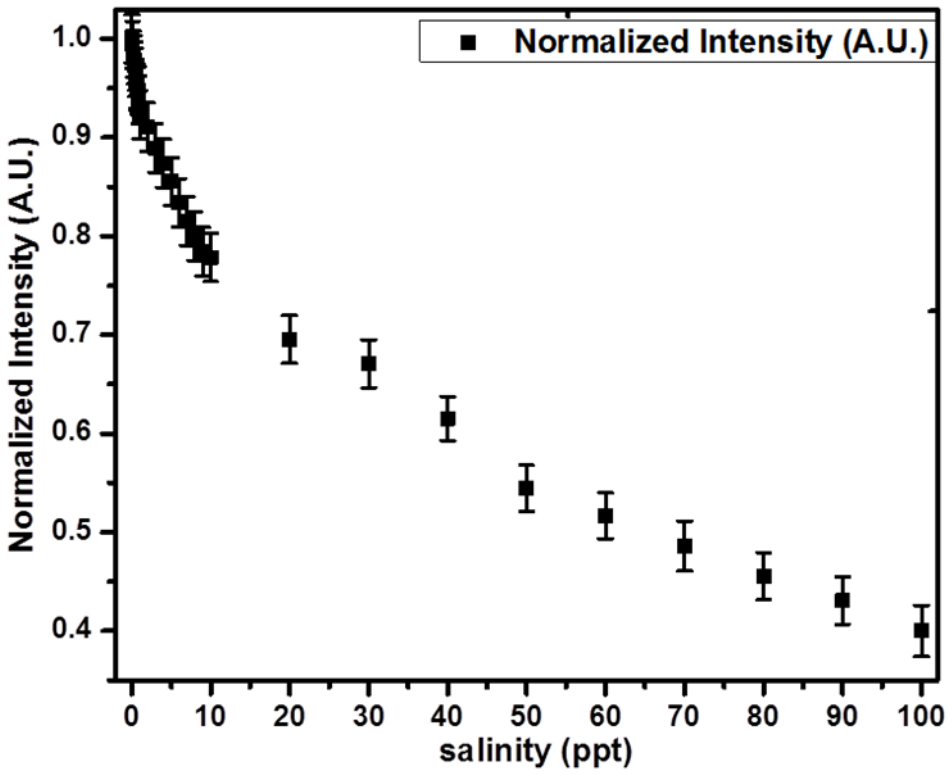

Figure 5.5: Response characteristic of the smartphone based fiber optic evanescent wave sensor in the salinity range 0 ppt to 100 ppt.

and accurately with the designed smartphone based fiber optic evanescent wave sensor. From the regression analysis, three calibration equations can be generated which are given as below.

The calibration equation in the salinity range 0 ppt to 1.0 ppt

$$\text{Salinity} = \frac{\text{Normalized intensity} - 1.0}{0.07} \tag{5.6}$$

The calibration equation in the salinity range 1.0 ppt to 10 ppt

$$\text{Salinity} = \frac{\text{Normalized intensity} - 0.94}{0.02} \tag{5.7}$$

and the calibration equation in the salinity range 10 ppt to 100 ppt

$$\text{Salinity} = \frac{\text{Normalized intensity} - 0.74}{0.004} \tag{5.8}$$

The above three calibration equations have been implemented in the designed smartphone application. Salinity of water samples outside the considered ranges

can be determined by successive dilution. After calibrating the device with the standard saline solutions, the performance of the sensor has been studies by evaluating its sensoristic parameters.

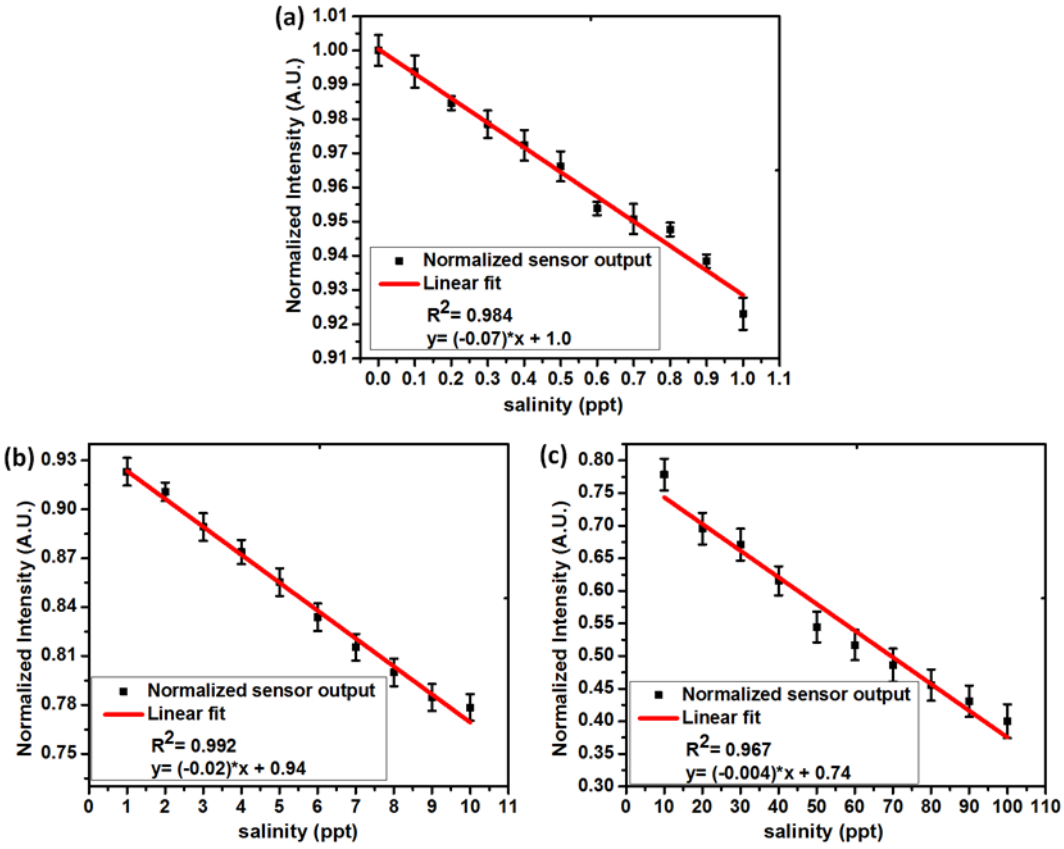

Figure 5.6: Response characteristic of the smartphone based fiber optic evanescent wave sensor in the salinity range (a) 0 ppt to 1.0 ppt, (b) 1 ppt to 10 ppt, and 10 ppt to 100 ppt.

5.7 Evaluation of different sensoristic parameters of the designed sensor

Parameters defining the device performance have been evaluated for the designed smartphone fiber optic evanescent wave sensor which are discussed below.

Sensitivity and resolution: The slope of the calibration curves has been considered to estimate the sensitivity. From figure 5.6 it is observed that the designed sensor is highly sensitive in the lower salinity range (0 ppt to 1.0 ppt) with sensitivity 0.07 A.U./ppt. The sensitivity is found to be decreasing in the higher

salinity range. In the salinity range 1.0 ppt to 10 ppt the sensitivity is found to be 0.02 A.U./ppt which is further decreased to 0.004 A.U./ppt in the salinity range 10 ppt to 100 ppt.

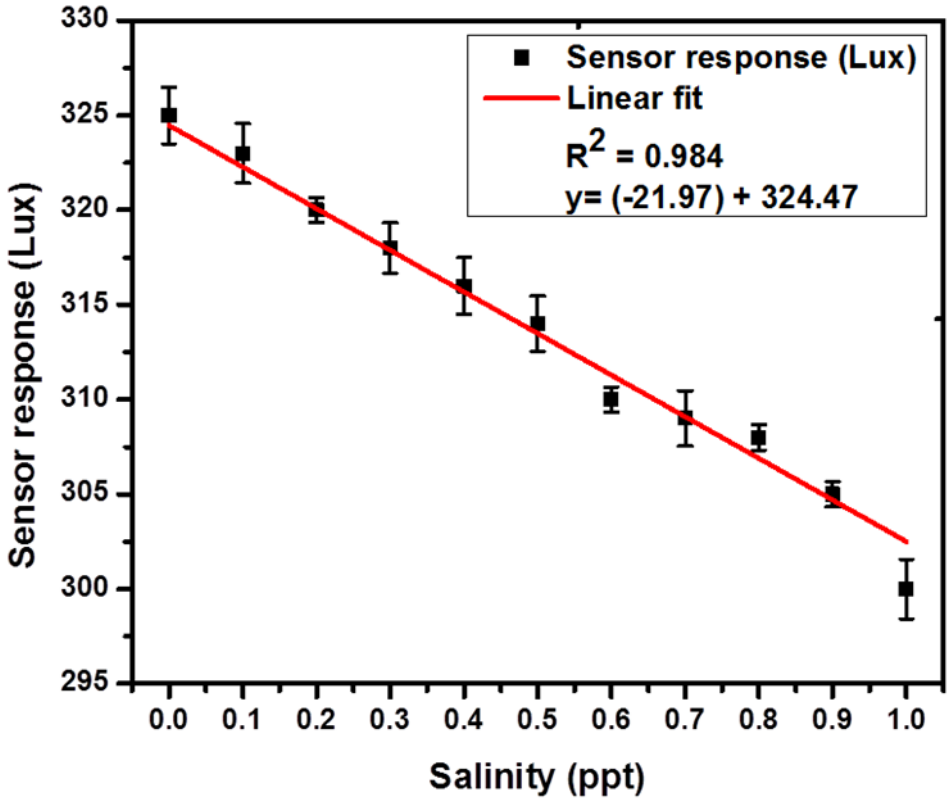

Figure 5.7: Response characteristics of the designed smartphone based fiber optic evanescent wave sensor in the salinity ranges 0 ppt to 1.0 ppt in terms of intensity units.

The resolution of the developed smartphone platform salinity sensor has been determined in the low salinity range 0 ppt to 1.0 ppt. by plotting its corresponding response characteristic shown in figure 5.6 (a) in the corresponding intensity units. Figure 5.7 shows the corresponding response characteristic in intensity units. The sensitivity of the designed smartphone sensor in terms of intensity unit is found to be $S = 21.97$ Lux/ppt. The resolution of the embedded ALS is $R_{ALS} = 0.01$ Lux, the corresponding resolution of the proposed smartphone salinity sensor can be determined by substituting the values of R_{ALS} and S in equation 3.10 of chapter 3 which yields the resolution as 4.55×10^{-4} ppt.

Determination of uncertainty in measurement: The uncertainty in measurements for the developed sensor has been evaluated. The sensor response measured

for samples in the salinity range 0.0 ppt to 1.0 ppt. For each sample, experiment data has been recorded for 10 consecutive times and the uncertainty in sensor reading is estimated. Figure 5.8 shows the characteristic uncertainty readings measured for all the considered samples. The maximum uncertainty reading is found to be below 0.01 ppt. This small uncertainty value clearly indicates that the salinity level variation as low as 0.1 ppt can be measured accurately and reliably with the designed sensor.

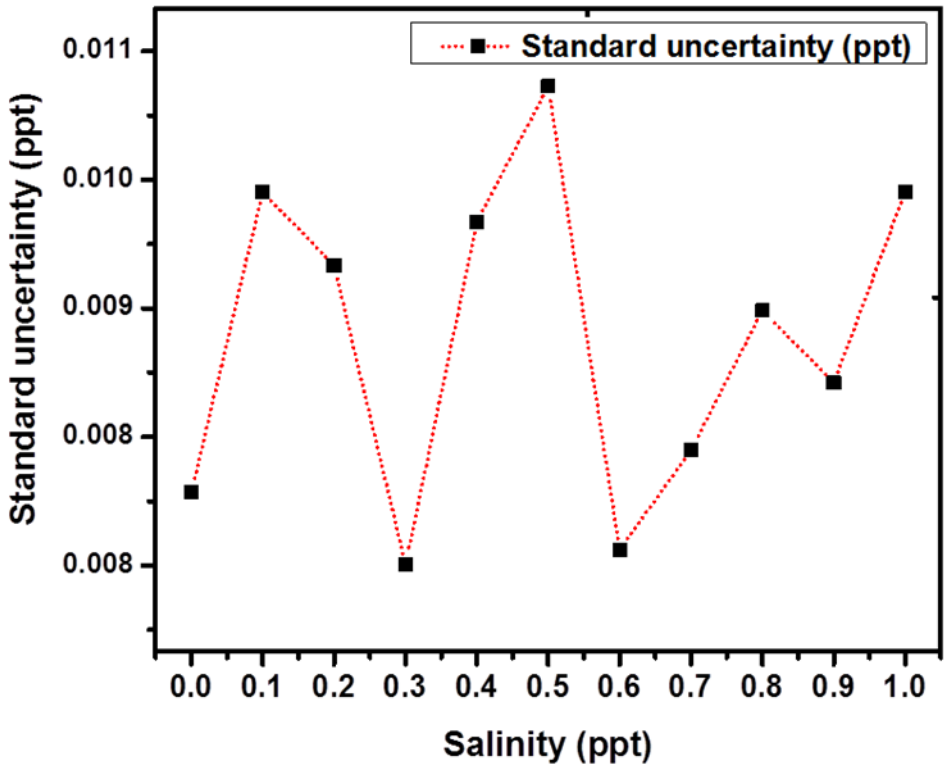

Figure 5.8: Uncertainty in measurement for both the sensing module for the salinity range 0 ppt to 1.0 ppt.

Stability analysis: For evaluation of stability characteristics 35 ppt saline standard has been considered as sample medium in the present study. Generally, the salinity level in environmental water is found in the range of 34 ppt to 35 ppt [36]. The sensor response for this specific salinity level has been observed for 2 hour by the designed sensor. The sensor response is recorded after every 10 minutes of interval. Figure 5.9 illustrates the time varying sensor characteristic curve which shows fairly stable sensor response. The maximum and minimum fluctuations in the normalized intensity reading are found to be 0.607 A.U. and 0.590 A.U.

respectively. Inserting these values in the calibration equation 5.8, it yields the maximum variation of salinity level occurring during this period of time is 4.25 ppt.

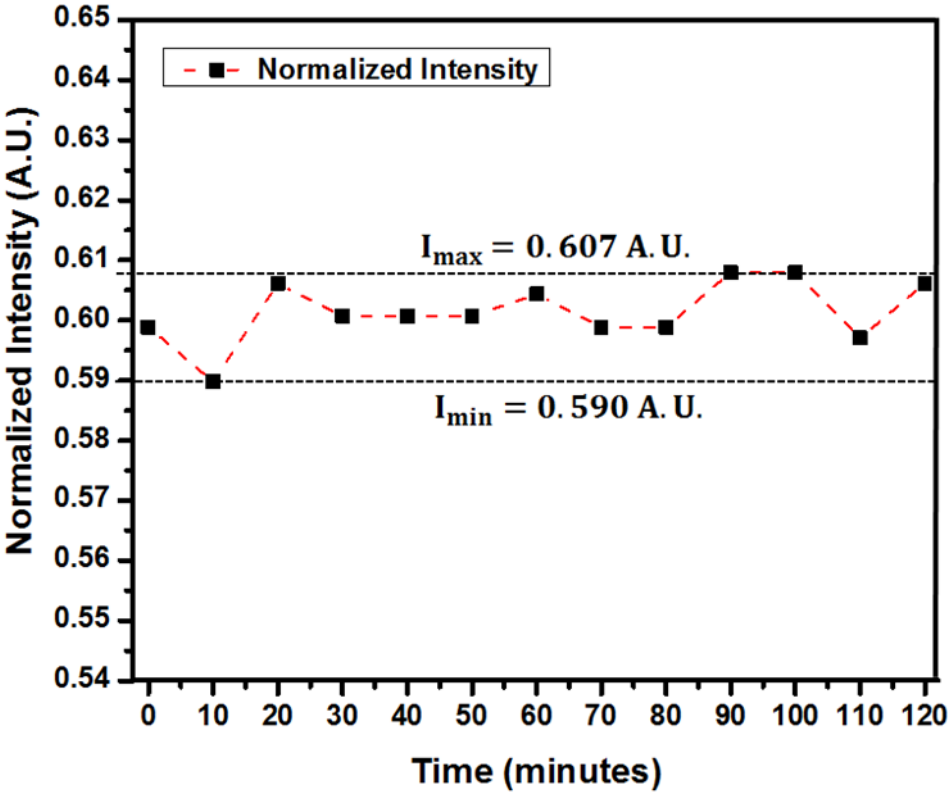

Figure 5.9: Stability measurement data the designed sensor for solution with salinity level of 35 ppt.

Evaluation of repeatability characteristics: To study the repeatability behaviour of the designed sensor 10 sample solutions in the salinity range 10 ppt to 100 ppt. Experimental data for these samples have been recorded for increasing and decreasing order of salinity level for 3 consecutive cycles. The repeatability characteristic of the designed sensors is shown in Figure 5.10. The characteristic curves clearly show that the designed sensor exhibits high repeatability behavior.These investigation has been performed for three weeks and similar responses have been observed in all trials.

Evaluation of range of the designed sensor: The coefficient of determination $R^2 = 0.984$ in the lower salinity range 0 ppt to 1.0 ppt and uncertainty in measurement yields for the considered range signifies that salinity level as low as 0.1 ppt can be determined accurately and precisely. Although, the sensitivity is found

to be less in the higher salinity, the coefficient of determination for this range is found to be $R^2 = 0.967$ which suggests that the designed sensor can still be used to measure high salinity levels in water. Thus, for the present smartphone platform fiber optic evanescent wave sensor, the sensing range or the dynamic range is 0.1 ppt to 100 ppt.

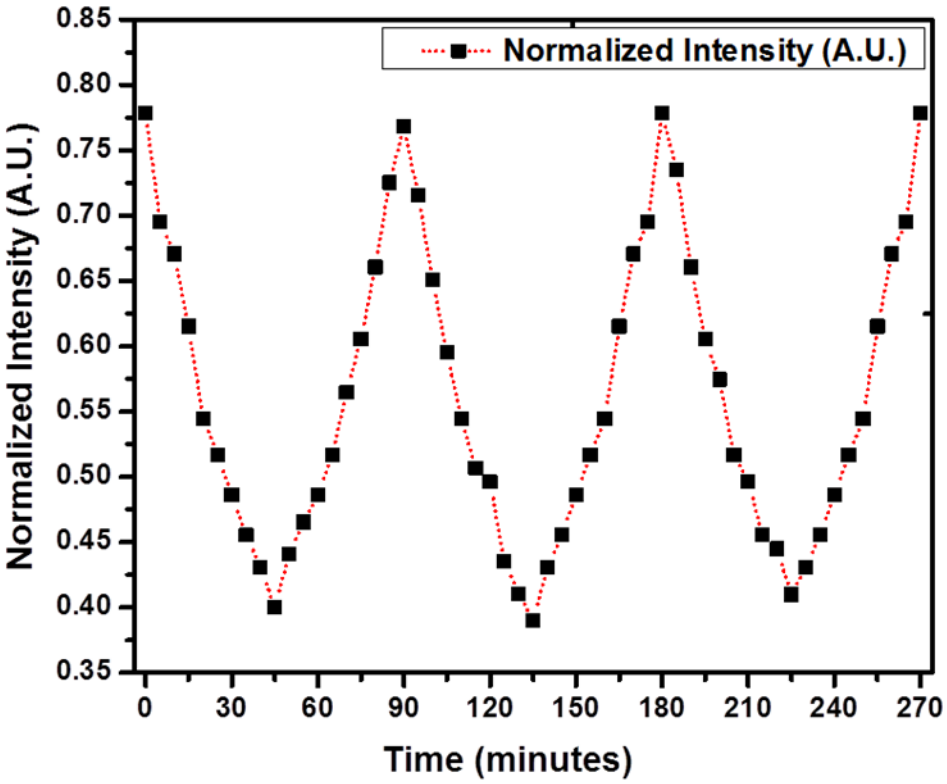

Figure 5.10: Repeatability characteristics of the designed sensor.

5.8 Comparison of the device performance with a standard tool

The performances of designed smartphone fiber optic sensor has been compared with the laboratory grade conductivity meter usually used for estimating the salinity level of sea water. The salinity levels of the prepared artificial sea salt samples have been initially measured with the standard conductivity meter (3540 Benchtop conductivity meter, Bibby Scientific) in μs/cm and then converted the value into corresponding salinity in ppt units by using an empirical conversion equation [23]. The salinity of the prepared samples were then measured by the designed

smartphone based sensor. Figure 5.11 describes the histogram representation of the experimental sensor data obtained from the smartphone based fiber optic sensor and with the standard tool. The error bars represent the standard deviations yield for five consecutive measurements of each sample. These experimental data clearly indicate that similar sensor response have been observed for both the sensors. A relatively larger variation has been observed in the conductivity meter reading which may be attributed due to the inaccuracy yield in the conversion formula.

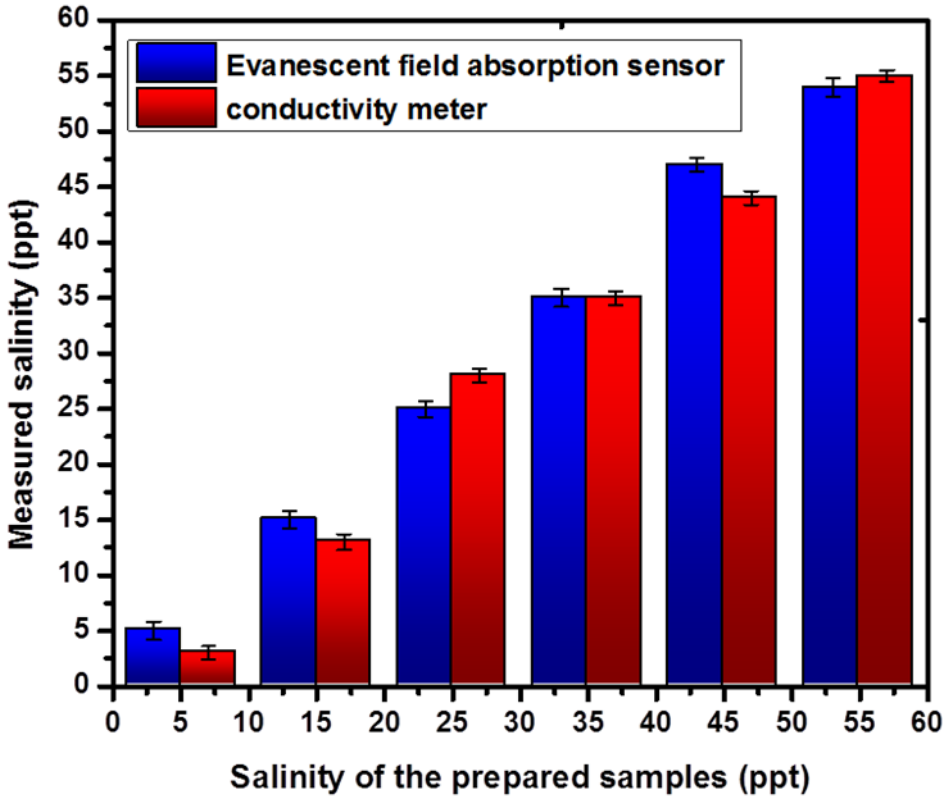

Figure 5.11: Histogram representation of comparison of salinity measurement of prepared water samples by the standard conductivity meter and by the designed smartphone salinity sensor.

5.9 Summary

In summary, the working of a low cost, robust, field portable smartphone platform fiber optic evanescent wave sensor has been demonstrated for monitoring of salinity level in water. The in-built LED flash and ALS of the smartphone have been

used as source and detector respectively, which eventually makes the proposed sensor as a stand-alone salinity sensor for in-situ determination of salinity level in water medium. An android application has been developed for detection and data analysis. Use of smartphone makes it possible for real time communication and data sharing from any remote location to the central water quality monitoring unit. The salinity values of different saline medium ranging from 0 to 100 ppt has been successfully measured by the designed sensing system. The present sensor module is suitable for salinity monitoring in oceanographic studies and also useful for household use. The performance of the sensor has been compared with that of a laboratory grade conductivity meter and good correlation has been observed. The designed smartphone based sensing system could emerge as an affordable solution for decentralized monitoring of water salinity in resource poor and remote regions.

References

[1] Salinity. Retrieved on 07 July, 2016 from http://www.epa.gov/national-aqua\tic-resource-surveys/indicators-salinity,2016.

[2] Wilson, T.R.S. Salinity and the major elements of sea water. *Chemical oceanography*, 1:365-413, 1975.

[3] Bear, J., Cheng, A.H.D., Sorek, S., Ouazar, D. and Herrera, I. *Seawater intrusion in coastal aquifers: concepts, methods and practices*, Springer Science and Business Media,1991.

[4] Calabrese, E.J. and Tuthill, R.W. The influence of elevated levels of sodium in drinking water on elementary and high school students in Massachusetts. *Science of the Total Environment*, 18:117-133, 1981.

[5] Khan, A., Mojumder, S.K., Kovats, S. and Vineis, P. Saline contamination of drinking water in Bangladesh. *Lancet*, 371(9610):385, 2008.

[6] Mabie, W.C., Pernoll, M.L. and Biswas, M.K. Chronic hypertension in pregnancy. *Obstetrics and gynecology*, 67(2):197-205, 1986.

[7] Coastal States of India. Retrieved on 07 July, 2016 from http://iomenvis.nic.in/index2.aspx?slid=758&sublinkid=119&langid=1&mid=1,2016.

[8] Alderman, M.H., Salt, blood pressure, and human health. *Hypertension*, 36(5):890-893, 2000.

[9] Hayashi, M. Temperature-electrical conductivity relation of water for environmental monitoring and geophysical data inversion. *Environmental monitoring and assessment*, 96(3):119-128, 2004.

[10] Meng, Q., Dong, X., Ni, K., Li, Y., Xu, B. and Chen, Z. Optical fiber laser salinity sensor based on multimode interference effect. *IEEE Sensors Journal*, 14(6):1813-1816, 2014.

[11] Rahman, H.A., Harun, S.W., Yasin, M. and Ahmad, H. Fiber-optic salinity sensor using fiber-optic displacement measurement with flat and concave mirror. *IEEE Journal of selected topics in quantum electronics*, 18(5):1529-1533, 2012.

[12] Rahman, H.A., Harun, S.W., Yasin, M., Phang, S.W., Damanhuri, S.S.A., Arof, H. and Ahmad, H. Tapered plastic multimode fiber sensor for salinity detection. *Sensors and Actuators A: Physical*, 171(2):219-222, 2011.

[13] Zhao, Y. and Liao, Y. Novel optical fiber sensor for simultaneous measurement of temperature and salinity. *Sensors and Actuators B: Chemical*, 86(1):63-67, 2002.

[14] Malarde, D., Wu, Z.Y., Grosso, P., de la Tocnaye, J.D.B. and Le Menn, M. High-resolution and compact refractometer for salinity measurements. *Measurement Science and Technology*, 20(1):015204, 2008.

[15] Ruddy, V., MacCraith, B.D. and Murphy, J.A. Evanescent wave absorption spectroscopy using multimode fibers. *Journal of Applied Physics*, 67(10):6070-6074, 1990.

[16] Gupta, B.D., Dodeja, H. and Tomar, A.K. Fibre-optic evanescent field absorption sensor based on a U-shaped probe. *Optical and Quantum Electronics*, 28(11):1629-1639, 1996.

[17] Khijwania, S.K. and Gupta, B.D. Maximum achievable sensitivity of the fiber optic evanescent field absorption sensor based on the U-shaped probe. *Optics Communications*, 175(1-3):135-137, 2000.

[18] Hecht, E. *Optics*, Addison-Wesley, San Francisco, 2002.

[19] Messica, A., Greenstein, A. and Katzir, A. Theory of fiber-optic, evanescent-wave spectroscopy and sensors. *Applied optics*, 35(13):2274-2284, 1996.

[20] Mathews, I.M. Refractive index and density. *Journal of the Franklin Institute*, 177(6):673-686, 1914.

[21] Gebhart, B. and Mollendorf, J.C. A new density relation for pure and saline water. *Deep Sea Research*, 24(9), pp.831-848, 1977.

[22] Defant, A. *Physical oceanography*,Pergamon,1961.

[23] Wilson, T.R.S. Salinity and the major elements of sea water. *Chemical oceanography*, 1:365-413, 1975.

[24] Lewis, E. The practical salinity scale 1978 and its antecedents. *IEEE Journal of Oceanic Engineering*, 5(1):3-8, 1980.